Anusandhanvallari
Vol 2023, No.1
December 2023
ISSN 2229-3388

Coupled Effects of Silica Fume and Steel-Fiber Geometry on the Mechanical and Elastic Performance of Concrete: Experimental Investigation, Statistical Interaction Analysis, and Predictive Modelling

[1]Mr. Sandeep Gaikwad, [2]Mr. Ajinkya Dharaskar, [3]Mr. Amey Khedikar

[1,2,3]Associate Professo Civil Engineering Department Tulsiramji Gaikwad Patil College of Engineering and Technology, Nagpur

Abstract: This study investigates the coupled effects of silica-fume replacement, steel-fibre dosage and fibre diameter on the mechanical, elastic and non-destructive performance of concrete through an integrated experimental and statistical framework. Silica fume was investigated at replacement levels of 4, 8 and 12%, with an additional 16% mixture used to establish the post-optimum response, while steel fibres were incorporated at 0.5, 1.0 and 1.5% using diameters of 0.5 and 1.0 mm. Performance was assessed through workability, cube and cylinder compressive strength, flexural strength, static and dynamic modulus of elasticity, ultrasonic pulse velocity (UPV), and compressive stress–strain behaviour, primarily at 28 and 90 days. Factorial analysis of variance and empirical regression were used to distinguish the relative contributions of the experimental variables and examine relationships among measured responses. Silica-fume incorporation increased cube compressive strength up to approximately 12% replacement, beyond which strength declined. The best-performing combination within the investigated domain contained 12% silica fume, 1.5% steel fibre and 1.0-mm-diameter fibres. At 90 days, this mixture achieved a cylinder compressive strength of 42.90 MPa, dynamic modulus of 48.30 GPa and UPV of 4752 m/s, corresponding to improvements of 20.34, 12.16 and 6.35%, respectively, relative to normal concrete. Its flexural strength reached 6.85 MPa, representing a 26.6% improvement over the corresponding reference concrete. Factorial ANOVA showed that silica-fume content exerted the dominant influence on compressive strength, whereas fibre dosage and fibre diameter had comparatively stronger effects on flexural performance. Higher-order interactions were not statistically significant, indicating that the observed improvements arose predominantly from cumulative main effects rather than a universal three-factor synergy. Representative empirical relationships produced coefficients of determination up to 0.977 within the investigated domain. The results demonstrate that multi-response assessment provides a more defensible basis for proportioning silica-fume steel-fibre concrete than compressive-strength optimisation alone, particularly where improvements in crack-sensitive behaviour must be balanced against increasing workability and admixture demand.

Keywords: Silica fume; Steel-fibre-reinforced concrete; Fibre dosage; Fibre diameter; Compressive strength; Flexural strength; Elastic modulus; Ultrasonic pulse velocity; Factorial ANOVA; Predictive modelling

1. Introduction

Concrete remains the dominant structural material used in modern infrastructure because of its versatility, availability and high compressive strength. However, its relatively low tensile capacity and brittle response after cracking continue to limit its performance, particularly in structural applications requiring improved toughness and crack resistance. This limitation can become more pronounced in high-strength concrete, where densification of the cementitious matrix increases compressive strength but does not necessarily provide a corresponding improvement in ductility. The development of concrete with a stronger matrix and improved resistance to crack initiation and propagation has therefore remained an important objective in cement-based materials research.

Silica fume is widely used as a supplementary cementitious material to improve the performance of concrete. Its very fine particles contribute through a combination of filler action and pozzolanic reaction, resulting in pore refinement and a denser cementitious matrix. The consumption of calcium hydroxide and formation of additional calcium silicate hydrate can improve the interfacial transition zone and contribute to higher strength and reduced permeability. These benefits, however, depend strongly on the replacement level. Excessive silica-fume incorporation can increase water demand, reduce workability and eventually produce diminishing improvements in mechanical performance. Consequently, identifying a suitable silica-fume dosage remains important when designing high-performance cementitious composites (Siddique 2011; Köksal et al. 2008).

Steel fibres address a different limitation of concrete. Rather than primarily strengthening the cementitious matrix, discrete fibres bridge developing cracks and allow stresses to be transferred across cracked regions. This mechanism restricts crack opening and delays unstable crack propagation, thereby improving tensile and flexural behaviour, toughness and post-cracking resistance. The effectiveness of steel fibres is governed not only by their dosage but also by their geometry. Fibre length, diameter and aspect ratio influence the available bond surface, anchorage and resistance to pull-out. Experimental evidence has shown that changes in fibre aspect ratio and volume fraction can significantly alter the mechanical response of steel-fibre-reinforced concrete, with particularly strong effects on tensile and flexural properties (Yazıcı, İnan, and Tabak 2007).

Combining silica fume and steel fibres therefore offers a potentially complementary approach to concrete modification. Silica fume strengthens and densifies the matrix, whereas steel fibres provide crack-bridging reinforcement. More importantly, these mechanisms are not completely independent. Modification of the matrix surrounding a fibre can influence fibre–matrix bond and stress transfer, while fibre geometry affects the manner in which stresses are redistributed once cracking begins. Earlier experimental studies have demonstrated that concrete performance is consequently influenced by the simultaneous effects of silica-fume content, fibre dosage and fibre geometry rather than by any single parameter in isolation (Bayasi and Soroushian 1997; Köksal et al. 2008; Nili and Afroughsabet 2010). Research on fibre–matrix interaction has further shown that silica fume can modify steel-fibre bond characteristics by altering the microstructure of the surrounding cementitious phase (Chan and Chu 2004; Wu, Shi, and Khayat 2016).

The incorporation of these materials also introduces an important fresh-state trade-off. Silica fume increases the surface area of the binder and consequently increases water demand, while steel fibres interfere with the movement and rearrangement of solid particles within fresh concrete. Increasing fibre dosage or changing fibre geometry may therefore reduce workability and complicate consolidation. Previous studies have reported reductions in slump with increasing fibre volume and aspect ratio (Yazıcı, İnan, and Tabak 2007). Adequate control of workability, including the appropriate use of chemical admixtures, is consequently necessary if improvements in hardened properties are to be achieved without introducing defects associated with inadequate compaction.

Although the combined behaviour of silica fume and steel fibres has been investigated for several decades, much of the available experimental literature has concentrated on conventional strength indicators such as compressive, splitting tensile and flexural strength. These parameters are essential, but they provide only a partial description of composite behaviour. Elastic stiffness, stress–strain response and ultrasonic pulse velocity provide complementary information concerning deformation characteristics and internal material quality. Moreover, the influence of fibre parameters is not necessarily identical across these responses. Steel-fibre content, for example, may have only a moderate influence on compressive strength while producing substantially greater changes in flexural behaviour and toughness (Köksal et al. 2008; Nili and Afroughsabet 2012).

Another limitation concerns how the effects of mixture variables are interpreted. Experimental studies frequently compare individual mixture averages even when silica-fume dosage, fibre content and fibre geometry are varied simultaneously. Such comparisons identify general trends but provide limited information regarding the magnitude and statistical significance of individual factors or the interactions between them. This is particularly relevant for silica-fume steel-fibre concrete because matrix densification, fibre concentration and fibre geometry influence different but interconnected mechanisms. More recent investigations have consequently introduced regression, response-surface methods and other statistical techniques to quantify these relationships and optimise fibre-reinforced concrete mixtures. Statistical modelling has demonstrated that silica-fume content, fibre volume and aspect ratio can be treated jointly to identify significant interactions and predict mechanical responses (Yazıcı, İnan, and Tabak 2007). Response-surface optimisation has subsequently extended this approach to simultaneous consideration of silica-fume content, fibre dosage and fibre aspect ratio.

The present study investigates these relationships through a systematic experimental and statistical assessment of concrete containing different silica-fume replacement levels and steel-fibre contents with different fibre geometries. The experimental programme evaluates both fresh and hardened behaviour, including workability and density, cube and cylinder compressive strength, flexural strength, static and dynamic modulus of elasticity, ultrasonic pulse velocity and stress–strain response at different curing ages. Rather than establishing merely whether silica fume and steel fibres improve concrete—which is already well documented—the study examines how silica-fume content, fibre dosage and fibre geometry jointly govern different performance indicators. Statistical interaction analysis and predictive modelling are incorporated to quantify the influence of the experimental variables and determine whether their effects remain consistent across strength, stiffness and nondestructive responses. The resulting framework is intended to provide a more integrated understanding of the mechanical and elastic performance of silica-fume concrete reinforced with steel fibres of different geometries.

2. Literature Review

Research on silica-fume steel-fibre-reinforced concrete has developed from separate investigations of matrix modification and fibre reinforcement toward studies examining their combined influence on mechanical behaviour. The available literature consistently shows that silica fume can improve matrix quality while steel fibres primarily influence cracking and post-cracking response. However, the magnitude of these benefits varies considerably with silica-fume replacement, fibre dosage and fibre geometry, making their interaction particularly important in designing high-performance concrete.

Bayasi and Soroushian (1997) provided one of the earlier systematic investigations of concrete containing both silica fume and steel fibres. Their results showed that silica fume improved several properties of high-strength concrete and that steel-fibre incorporation altered its mechanical response. The study was important in demonstrating the feasibility of combining matrix densification with discrete fibre reinforcement, but it did not establish a comprehensive multi-variable framework capable of separating the individual and interactive effects of silica-fume content and fibre characteristics. Subsequent research increasingly focused on these variables and their combined influence.

The role of fibre geometry was examined more directly by Yazıcı, İnan, and Tabak (2007), who investigated steel fibres with aspect ratios of 45, 65 and 80 at volume fractions of 0.5, 1.0 and 1.5%. Their results demonstrated that both aspect ratio and fibre volume influenced the mechanical properties of steel-fibre-reinforced concrete. The improvement was particularly evident in properties associated with tensile and flexural behaviour, whereas compressive strength was less sensitive to fibre addition. Their regression analysis further demonstrated that fibre parameters could be related quantitatively to concrete properties. Nevertheless, silica-fume content was not treated as an interacting experimental factor, leaving the influence of matrix modification outside the principal factorial relationship.

A closer experimental configuration was subsequently reported by Köksal et al. (2008), who investigated high-strength concrete containing different silica-fume contents together with steel fibres of two aspect ratios. Their study demonstrated that silica-fume replacement, fibre content and fibre geometry collectively affected concrete performance. Silica fume contributed primarily through improvement of the cementitious matrix, while steel fibres produced more pronounced improvements in toughness-related behaviour. The results also indicated that increasing fibre aspect ratio could enhance reinforcement efficiency. This study remains particularly relevant because it established that the response of the composite cannot be described adequately by considering silica fume and steel fibres independently.

Nili and Afroughsabet (2010) extended this understanding by examining the combined influence of silica fume and steel fibres on mechanical properties and impact resistance. Their findings showed that fibre reinforcement was especially beneficial for properties governed by cracking and energy absorption. In a subsequent investigation, Nili and Afroughsabet (2012) assessed silica-fume concrete reinforced with steel fibres and reported improvements in compressive and tensile-related properties with fibre incorporation. These studies reinforced an important distinction: silica fume and steel fibres do not contribute equally to every response. Matrix modification may substantially affect compressive strength, while fibre reinforcement generally has a stronger influence on tensile, flexural, impact and post-cracking behaviour.

The interaction between silica fume and steel fibres can be explained partly through changes occurring at the fibre–matrix interface. Chan and Chu (2004) investigated steel-fibre bond characteristics in silica-fume-containing reactive powder concrete and demonstrated that silica fume influenced fibre bonding behaviour. Wu, Shi, and Khayat (2016) subsequently examined microstructure development and steel-fibre bonding in ultra-high-strength cementitious materials. Their work showed that silica-fume content affected the microstructure surrounding the fibre and consequently the fibre–matrix bond. These observations are significant because the contribution of a steel fibre depends on the transfer of stress from the cementitious matrix to the fibre before and after cracking. Fibre geometry and matrix quality should therefore be regarded as coupled parameters rather than independent characteristics.

The benefits obtained in the hardened state are accompanied by changes in fresh behaviour. Increasing silica-fume content generally raises water demand because of its high specific surface area, whereas steel fibres restrict the mobility of fresh concrete and increase resistance to flow. Köksal et al. (2008) observed deterioration in workability with increasing fibre and silica-fume contents, while Yazıcı, İnan, and Tabak (2007) also reported changes in fresh properties associated with fibre dosage and aspect ratio. This creates a practical constraint on fibre-reinforced silica-fume concrete: a mixture producing superior hardened properties may require greater chemical-admixture dosage to maintain adequate placement and consolidation. Workability therefore needs to be considered alongside mechanical optimisation rather than treated independently.

Although compressive strength has dominated much of the literature, flexural behaviour provides a more direct indication of the contribution of fibres. Steel fibres bridge cracks that develop in the tensile zone and continue transferring stresses after matrix cracking. Song and Hwang (2004) reported substantial improvements in the mechanical behaviour of high-strength concrete with increasing steel-fibre content, while later investigations have confirmed that fibre geometry, dosage and matrix strength govern the magnitude of the resulting flexural enhancement. Crack bridging also changes the failure mechanism from rapid localisation toward more distributed cracking, although the effectiveness of this mechanism depends on fibre anchorage and orientation.

Elastic properties and nondestructive measurements have received comparatively less attention than strength. Dynamic and static modulus measurements provide information on stiffness and deformation, while ultrasonic pulse velocity (UPV) is sensitive to the continuity and internal quality of the concrete matrix. Yazıcı, İnan, and Tabak (2007) incorporated UPV into their assessment and found that the response of UPV to fibre parameters differed from the response observed for mechanical strength. This distinction is important because the introduction of steel fibres may strongly improve crack resistance without producing a proportional increase in pulse velocity or elastic modulus. Evaluating several response variables simultaneously can therefore reveal performance trade-offs that are obscured when optimisation is based solely on compressive strength.

More recent studies have shifted toward quantitative modelling of these multivariable relationships. Statistical approaches, particularly regression and response surface methodology, have been applied to fibre-reinforced concrete to quantify the influence of mixture parameters and determine optimum combinations. Studies using silica-fume content, fibre volume and fibre aspect ratio as independent variables have demonstrated that interaction and quadratic effects can be statistically significant and that optimum conditions depend on the selected response. Machine-learning-based models have also been developed for predicting the compressive and flexural strength of steel-fibre-reinforced concrete using mixture composition and fibre characteristics as predictors. These developments represent a transition from descriptive comparison toward predictive interpretation, but they also show that models developed for one mechanical property cannot automatically be assumed to represent other performance indicators.

2.1 Research gap and contribution of the present study

Despite extensive research on silica fume and steel-fibre-reinforced concrete, three limitations remain relevant to the present investigation. First, many studies have concentrated on a limited group of conventional mechanical properties, most commonly compressive, splitting tensile and flexural strength. Fewer experimental programmes have simultaneously considered strength, static and dynamic stiffness, stress–strain behaviour and nondestructive indicators such as UPV across a common set of silica-fume and fibre variables. Consequently, the extent to which the same mixture parameters govern different categories of concrete response remains insufficiently resolved.

Second, fibre dosage and fibre geometry are frequently investigated independently or under a fixed matrix composition. Studies that incorporate silica fume together with multiple fibre dosages and geometries have established important trends (Köksal et al. 2008), but the combined experimental space remains relatively limited when multiple curing ages and mechanical, elastic and nondestructive responses are considered together. The interaction between matrix modification and fibre reinforcement therefore warrants evaluation across a broader set of performance indicators rather than through a single optimum-strength criterion.

Third, much of the earlier experimental literature relies on comparisons between mixture averages. Although recent response-surface, regression and machine-learning studies have improved predictive capability, there remains value in linking statistical interaction analysis directly with a controlled experimental programme containing replicate observations. Such an approach allows the significance and magnitude of silica-fume content, fibre dosage and fibre geometry to be evaluated alongside the experimentally observed behaviour.

The present study addresses these limitations through an integrated experimental-statistical assessment of silica-fume concrete reinforced with steel fibres of different geometries and dosages. Multiple curing ages and response variables are considered, including cube and cylinder compressive strength, flexural strength, static and dynamic modulus of elasticity, stress–strain behaviour and ultrasonic pulse velocity. Factor effects and interactions are subsequently examined statistically and incorporated into predictive relationships. This approach enables the influence of silica-fume content, fibre dosage and fibre geometry to be compared across different performance measures and provides a basis for identifying combinations that offer balanced mechanical and elastic performance rather than maximising a single response.

3. Materials and Methodology

3.1 Experimental framework

The experimental programme was designed to examine the combined influence of silica-fume replacement, steel-fibre dosage and fibre geometry on the fresh, mechanical and elastic behaviour of concrete. Normal concrete without silica fume or steel fibres was used as the reference mixture. Silica fume was incorporated at replacement levels of 4, 8 and 12%, while steel fibres were introduced at 0.5, 1.0 and 1.5%. Two fibre diameters, 0.5 and 1.0 mm, were investigated. These levels generated a systematic experimental matrix through which the effects of matrix modification, fibre concentration and fibre geometry could be evaluated individually and in combination. The experimental record also contained silica-fume-only mixtures, allowing the contribution of silica fume to be distinguished from the additional effect produced by fibre reinforcement.

Fibre diameter rather than aspect ratio was retained as the geometrical variable in the present analysis because the available experimental record identifies fibre diameter explicitly but does not provide sufficient information to establish fibre length consistently. Consequently, no unverified aspect ratio was assigned retrospectively.

The principal experimental factors were silica-fume replacement (SF), steel-fibre volume fraction (Vf), fibre diameter (df), and curing age (t). The measured responses included slump, fresh and dry density, cube and cylinder compressive strength, flexural strength, static and dynamic modulus of elasticity, ultrasonic pulse velocity (UPV), and stress-strain behaviour. Tests at different ages were retained where observations were available in the original dataset.

3.2 Constituent materials and mixture design

The concrete consisted of cementitious binder, fine aggregate, coarse aggregate, water, silica fume, steel fibres and a chemical superplasticizer. Silica fume was used as a partial replacement for the cementitious component rather than as an additional binder. The exact cement grade, aggregate grading, water-to-binder ratio and constituent quantities are not recoverable from the available experimental record and are therefore not assigned retrospectively in this paper. This avoids introducing material characteristics that cannot be verified from the original experimental programme.

The control mixture contained neither silica fume nor steel fibres. The silica-fume series contained 4, 8 and 12% replacement, after which steel fibres were incorporated at 0.5, 1.0 and 1.5% for each silica-fume level. Separate experimental series were produced using the 0.5- and 1.0-mm-diameter fibres.

A chemical superplasticizer was used to compensate for the progressive reduction in workability associated with silica fume and fibre addition. The available records show that the required dosage generally increased with both silica-fume and fibre contents. For mixtures containing the 1.0-mm fibre series, the recorded superplasticizer dosage ranged from 0.9% at 4% silica fume and 0.5% fibre to 1.8% at 12% silica fume and 1.5% fibre. The corresponding slump remained within approximately 22-24 mm. This adjustment was necessary because fibre contents above approximately 0.5% produced a pronounced reduction in mixture workability unless fluidity was modified using superplasticiser.

3.3 Mixing, casting and curing

Concrete constituents were proportioned for each experimental combination, followed by incorporation of silica fume at the specified replacement level. Steel fibres were subsequently distributed through the concrete at the required volume fraction. Particular care was required during fibre addition to minimise fibre agglomeration and obtain a reasonably uniform distribution within the matrix.

Because the surviving experimental record does not preserve the original mixer sequence or individual mixing durations, these parameters are not reconstructed numerically. The procedure was instead governed by the requirement to obtain a homogeneous mixture before casting.

Fresh concrete was placed into the appropriate moulds and compacted using vibration. The original programme adopted a vibration period of approximately 15 ± 5 s as a practical criterion for achieving adequate consolidation. After casting, specimens were cured until the specified testing ages. The principal hardened-property comparisons were conducted at 28 and 90 days, while earlier-age results were retained for tests for which such observations were available.

Cylinder specimens used for compressive, elastic and stress-strain measurements were 150 mm in diameter and 300 mm in height. At least three individual measurements were available for the principal response combinations, and statistical analyses were performed using the individual observations wherever replicate data were recoverable rather than using only reported averages.

3.4 Fresh concrete properties

Workability was evaluated using the slump test immediately after mixing. The response was interpreted together with superplasticizer demand because maintaining a workable mixture became progressively more difficult as the solid surface area and fibre content increased.

The experimental data show slump values generally remaining above approximately 20 mm after superplasticizer adjustment. Fresh density was also determined for the different silica-fume/fibre combinations. For example, the 1.0-mm fibre series produced wet densities of approximately 2379-2407 kg/m³ over the investigated experimental domain. Fresh-state results were subsequently compared with hardened properties to determine whether mixtures producing greater strength or stiffness incurred a significant workability penalty.

3.5 Mechanical testing

3.5.1 Compressive strength

Compressive strength was determined for both cube and cylindrical specimens at the specified curing ages. Cylinder testing was conducted using a 2000-kN compression testing machine, with the 150 × 300 mm specimens tested following the procedure reported with reference to IS 516.

Compressive strength was calculated from the maximum applied load and loaded cross-sectional area:

$$f_c = \frac{P_{max}}{A} \quad (1)$$

where fc is the compressive strength (MPa), Pmax is the maximum compressive load (N), and A is the loaded cross-sectional area (mm²).

Percentage improvement relative to the reference concrete was determined as:

$$\Delta f_c(\%) = \frac{f_{c,i} - f_{c,0}}{f_{c,0}} \times 100 \quad (2)$$

where fc,i represents the strength of a modified mixture and fc,0 is the corresponding reference-concrete strength. Individual replicate measurements were retained before calculating mean strengths.

3.5.2 Flexural strength

Flexural testing was performed to quantify the influence of fibre reinforcement on the tensile-controlled response of concrete. The modulus of rupture was calculated according to the loading configuration used in the original programme. For third-point loading, the general expression is:

$$f_r = \frac{PL}{bd^2} \quad (3)$$

where fr is the flexural strength (MPa), P is the failure load (N), L is the effective span (mm), b is the specimen width (mm), and d is the specimen depth (mm). Three observations were retained for the principal fibre/silica-fume combinations at each age wherever available.

3.6 Stress-strain behaviour and static modulus of elasticity

Stress-strain behaviour was measured using 150 × 300 mm cylinders tested under axial compression. A compressometer equipped with dial gauges was attached to the cylinder to record axial deformation during loading. Stress and axial strain were calculated as:

$$\sigma = \frac{P}{A} \quad (4)$$

$$\varepsilon = \frac{\Delta L}{L_0} \quad (5)$$

where σ is the axial stress, P is the applied load, A is the specimen cross-sectional area, ε is the axial strain, ΔL is the measured change in gauge length, and L0 is the initial gauge length.

Stress-strain curves were generated for normal concrete, silica-fume concrete and silica-fume concrete containing different fibre dosages and diameters at 28 and 90 days. The original testing programme reports determination of static modulus with reference to the ACI 318 procedure used at the time of testing. The secant modulus can be represented generally by:

$$E_s = \frac{\sigma_2 - \sigma_1}{\varepsilon_2 - \varepsilon_1} \quad (6)$$

where Es is the static modulus of elasticity, and (σ1, ε1) and (σ2, ε2) define the selected stress-strain interval.

3.7 Ultrasonic pulse velocity and dynamic modulus of elasticity

Nondestructive assessment was conducted using ultrasonic pulse velocity. The pulse travelled through the 300-mm path length of the cylindrical specimens, and the transit time was measured for each specimen. UPV was calculated as:

$$V = \frac{L}{T} \quad (7)$$

where V is ultrasonic pulse velocity (m/s), L is the transmission path length (m), and T is the measured transit time (s). The source reports UPV testing according to IS 13311 (Part 1):1992. UPV was analysed alongside compressive strength and modulus rather than being treated as an isolated quality indicator.

Dynamic modulus of elasticity was also determined for the cylindrical specimens. The experimentally reported values were retained as the primary dataset. The relationship between dynamic modulus, compressive strength and UPV was subsequently examined statistically to determine whether changes in matrix/fibre composition produced consistent changes across destructive and nondestructive responses.

3.8 Statistical analysis and predictive modelling

Statistical analysis was designed to move beyond simple comparison of mixture averages. Individual replicate measurements were used wherever available. For each experimental combination, the arithmetic mean, standard deviation and coefficient of variation were calculated as:

$$\bar{x} = \frac{1}{n} \Sigma x_i \quad (8)$$

$$s = \sqrt{\frac{\Sigma (x_i - \bar{x})^2}{n-1}} \quad (9)$$

$$CV(\%) = \frac{s}{\bar{x}} \times 100 \quad (10)$$

where xi is an individual observation and n is the number of replicates.

For response datasets containing the complete experimental combinations, a general linear model/factorial analysis of variance was used to assess the influence of silica-fume content, fibre dosage and fibre diameter, together with statistically estimable interaction terms. Curing ages were analysed as separate response stages where this provided a clearer interpretation and avoided treating age-related strength development as equivalent to a mixture-design factor.

The general factorial representation was:

$$Y = \beta_0 + \beta_1 SF + \beta_2 V_f + \beta_3 d_f + \beta_{12}(SF \times V_f) + \beta_{13}(SF \times d_f) + \beta_{23}(V_f \times d_f) + \varepsilon \quad (11)$$

where Y represents the measured response, SF is silica-fume content, Vf is fibre volume fraction, df is fibre diameter, β0 is the intercept, βi are main-effect coefficients, βij are interaction coefficients, and ε represents random error.

Statistical significance was assessed at $p < 0.05$. Main effects were not interpreted independently where statistically meaningful interaction terms were present. Effect magnitude and interaction plots were used alongside significance testing so that practical changes in concrete performance were not judged solely from p-values.

Predictive regression models were subsequently developed for response variables with sufficient observations. Where justified by the data structure, second-order terms were considered to represent nonlinear responses:

$$Y = \beta_0 + \Sigma\beta_i X_i + \Sigma\beta_{ii} {X_i}^2 + \Sigma\beta_{ij} X_i X_j + \varepsilon \quad (12)$$

Model adequacy was assessed using the coefficient of determination (R^2), adjusted coefficient of determination (adjusted R^2), root-mean-square error (RMSE), and mean absolute error (MAE):

$$R^2 = 1 - \frac{\Sigma(y_i - \hat{y}_i)^2}{\Sigma(y_i - \bar{y})^2} \quad (13)$$

$$RMSE = \sqrt{\frac{1}{n}\Sigma(y_i - \hat{y}_i)^2} \quad (14)$$

$$MAE = \frac{1}{n}\Sigma|y_i - \hat{y}_i| \quad (15)$$

where yi and ŷi are the experimental and predicted values, respectively. Residual normality, constant variance and influential observations were examined before accepting the final regression relationships. Predictive performance was therefore evaluated from both goodness-of-fit and residual behaviour rather than from R^2 alone.

Where several response variables exhibited conflicting optima, optimisation was based on balanced performance rather than maximum compressive strength alone. This was particularly important because the effects of steel fibres on compressive strength, flexural behaviour, stiffness and UPV were not expected to be identical. The final optimum combination was therefore selected only after considering the statistical and engineering significance of the principal mechanical and elastic responses.

4. Results and Discussion

4.1 Fresh-state behaviour and workability

The incorporation of silica fume and steel fibres produced a clear reduction in the workability of the concrete, and this effect became progressively stronger as the dosage of either constituent increased. Silica fume alone increased the demand for superplasticizer because of its high specific surface area and the associated increase in water demand. In the experimental programme, increasing the silica-fume replacement from 4 to 16% required the superplasticizer dosage to increase from approximately 0.75 to 1.40% to maintain a slump above 20 mm. This behaviour is consistent with previous observations that silica fume can substantially increase the water and admixture demand of concrete because of its extremely fine particle size (Köksal et al. 2008; Saba et al. 2021).

The loss of workability became more pronounced when steel fibres were introduced. For the 0.5-mm-diameter fibre series, the superplasticizer dosage increased from 0.80% for the mixture containing 4% silica fume and 0.5% fibre to 1.60% for the mixture containing 12% silica fume and 1.5% fibre. Despite the increased admixture dosage, slump decreased from 28 to approximately 24 mm. The corresponding 1.0-mm fibre mixtures required still higher superplasticizer contents, ranging from approximately 0.90 to 1.80%, while slump remained within the relatively narrow range of 22–24 mm.

Table 1. Fresh-state response of selected silica-fume/steel-fibre mixtures

Silica fume (%)	Fibre dosage (%)	Fibre diameter (mm)	Superplasticizer (%)	Slump (mm)
4	0.5	0.5	0.80	28
4	1.0	0.5	0.90	26
4	1.5	0.5	1.00	25
8	0.5	0.5	1.00	26
8	1.0	0.5	1.20	25
8	1.5	0.5	1.40	26
12	0.5	0.5	1.20	26
12	1.0	0.5	1.40	23
12	1.5	0.5	1.60	24

Note: Values are taken from the original experimental dataset.

The reduction in slump can be attributed to two simultaneous mechanisms. First, silica fume increases the total surface area that must be wetted and consequently raises the water demand of the cementitious system. Second, the fibres mechanically restrict the movement of aggregate particles and increase internal resistance to flow. At higher fibre concentrations, fibre-fibre and fibre-aggregate interactions further increase the apparent viscosity of the fresh concrete. Similar behaviour has been reported for steel-fibre-reinforced concretes, where increasing fibre content generally reduces workability even when the hardened mechanical properties improve.

An important point is that the decrease in workability did not translate into a corresponding deterioration in hardened properties. This indicates that the increasing superplasticizer dosage was sufficient to maintain workable and adequately compactable mixtures throughout the experimental range. The wet density remained between approximately 2367 and 2407 kg/m³ across the investigated mixtures, suggesting that no major loss of consolidation occurred. Nevertheless, the rapid increase in admixture requirement at the highest silica-fume and fibre contents represents a practical limitation. The mixture giving the highest mechanical performance therefore also imposed the greatest fresh-state demand.

Anusandhanvallari
Vol 2023, No.1
December 2023
ISSN 2229-3388

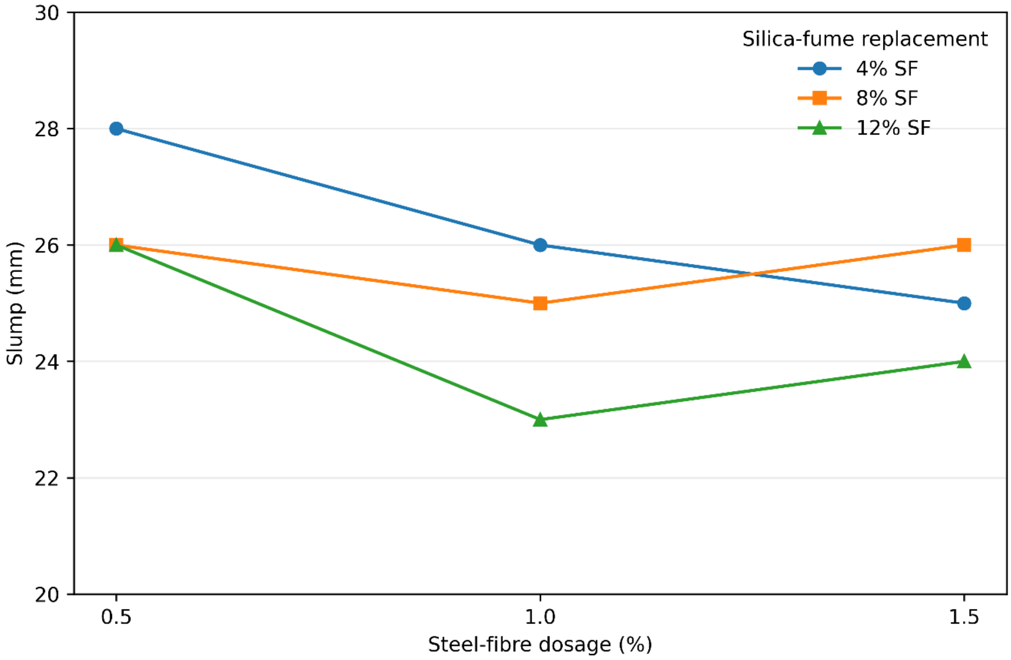

Figure 1 Effect of steel-fibre dosage and silica-fume replacement on the slump of concrete containing 0.5-mm-diameter steel fibres

As shown in Fig. 1, slump generally decreased with increasing steel-fibre dosage, with the reduction becoming more pronounced at higher silica-fume replacement levels. The trend highlights the combined influence of increased matrix surface area and fibre-induced resistance to flow, particularly for the 12% silica-fume mixtures.

4.2 Effect of silica fume on compressive strength

The silica-fume-only mixtures were first examined separately to distinguish the effect of matrix modification from that produced subsequently by steel-fibre reinforcement. A consistent increase in cube compressive strength was observed when the silica-fume replacement increased from 0 to 12%. Increasing the replacement further to 16%, however, caused the strength to decline. The existence of this turning point is important because it demonstrates that the beneficial effect of silica fume was not simply proportional to dosage.

At 28 days, the reference concrete produced an average cube compressive strength of 40.37 MPa when superplasticizer was used. The corresponding strengths at 4, 8 and 12% silica-fume replacement were 43.38, 44.88 and 45.18 MPa, respectively. At 16% replacement, strength decreased to 44.54 MPa. A similar response was observed at 90 days: the strength increased to 45.53, 47.22 and 47.48 MPa at 4, 8 and 12% silica fume, respectively, but declined to 46.73 MPa at 16%.

Table 2. Effect of silica-fume replacement on cube compressive strength

Silica fume (%)	28-day strength (MPa)	90-day strength (MPa)
0	40.37	42.16
4	43.38	45.53
8	44.88	47.22

Anusandhanvallari
Vol 2023, No.1
December 2023
ISSN 2229-3388

12	**45.18**	**47.48**
16	44.54	46.73

Note: The 0% values correspond to the normal concrete containing the reported superplasticizer dosage. The 16% mixture was investigated to identify the post-optimum trend.

The improvement up to 12% can reasonably be associated with the combined filler and pozzolanic effects of silica fume. Fine silica-fume particles fill spaces within the cementitious matrix while the pozzolanic reaction consumes calcium hydroxide and contributes additional calcium-silicate-hydrate phases. These mechanisms generally produce a denser paste and a stronger interfacial transition zone. Systematic reviews of silica-fume cementitious composites similarly show that compressive strength generally rises up to an optimum replacement level before excessive replacement can become counterproductive.

The decline from 12 to 16% is therefore particularly relevant. Once silica-fume replacement exceeds the level at which its filler and pozzolanic contributions compensate for the reduction in Portland cement, further replacement does not necessarily provide additional strength. Higher silica-fume contents also impose greater water and superplasticizer demand. The present experimental programme consequently identifies **approximately 12% silica fume as the optimum replacement within the investigated material system**, rather than implying that further increases would continue to improve performance. The original experimental record likewise identifies 12% as the point beyond which cube strength began to decline. As illustrated in Fig. 2, cube compressive strength increased progressively with silica-fume replacement up to 12% at both curing ages, after which a moderate decline was observed at 16%. The similar trend at 28 and 90 days confirms that the optimum around 12% was maintained with curing age rather than being restricted to early-age strength development.

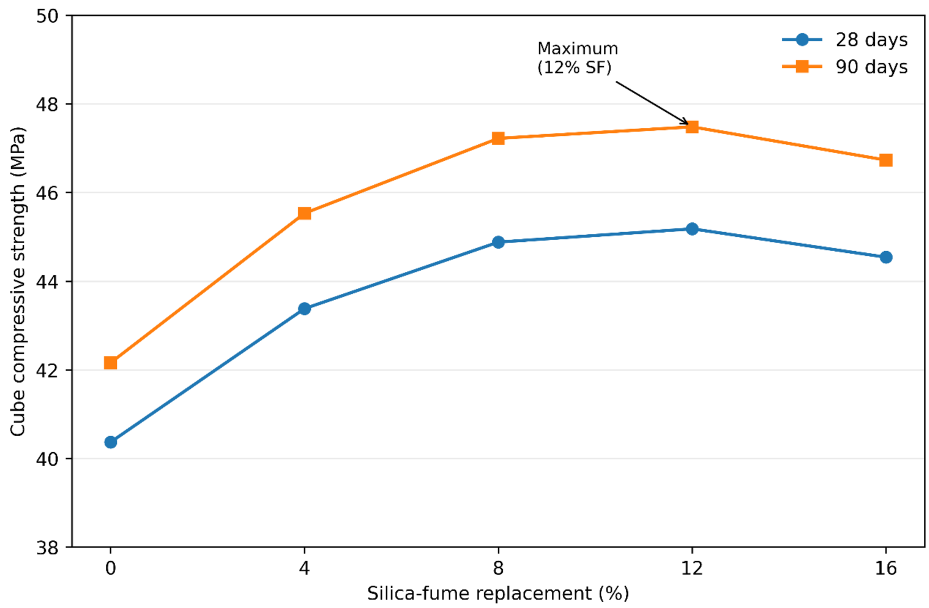

Figure 2 Effect of silica-fume replacement on cube compressive strength at 28 and 90 days.

4.3 Combined influence of silica fume, fibre dosage and fibre diameter on compressive strength

The introduction of steel fibres produced a further improvement over the silica-fume-only concrete. Unlike the pronounced influence of silica fume on matrix strength, however, the contribution of steel fibres to compressive strength was more gradual. The primary role of fibres under compression is not to increase the intrinsic strength of the cement paste but to restrain crack propagation and lateral deformation as internal microcracks develop.

Across the investigated mixtures, compressive strength generally increased with fibre dosage from 0.5 to 1.5%. The effect was also influenced by fibre diameter. The 1.0-mm fibre series generally produced greater improvements than the corresponding 0.5-mm series, particularly at higher silica-fume and fibre contents.

The cylinder results illustrate this interaction particularly clearly. At 90 days, normal concrete developed a compressive strength of 35.65 MPa. With 12% silica fume and 1.0-mm fibres, strength increased to 40.67 MPa at 0.5% fibre, 42.26 MPa at 1.0% fibre and 42.90 MPa at 1.5% fibre. These values correspond to improvements of 14.08, 18.54 and 20.34%, respectively, relative to normal concrete.

Table 3. Effect of fibre dosage on 90-day cylinder properties for the 1.0-mm fibre series

SF (%)	Fibre (%)	Compressive strength (MPa)	Increase (%)	Dynamic modulus (GPa)	Increase (%)	UPV (m/s)	Increase (%)
0	0	35.65	–	43.06	–	4468	–
4	0.5	38.90	9.12	45.92	6.64	4602	2.99
4	1.0	39.84	11.75	46.94	9.01	4644	3.93
4	1.5	40.64	13.99	47.05	9.26	4674	4.61
8	0.5	40.14	12.59	46.81	8.71	4634	3.72
8	1.0	41.88	17.48	47.82	11.05	4695	5.08
8	1.5	42.56	19.38	48.20	11.93	4729	5.84
12	0.5	40.67	14.08	47.14	9.47	4661	4.32
12	1.0	42.26	18.54	47.92	11.28	4719	5.62
12	1.5	**42.90**	**20.34**	**48.30**	**12.16**	**4752**	**6.35**

Note: Percentage increases are relative to the corresponding normal concrete.

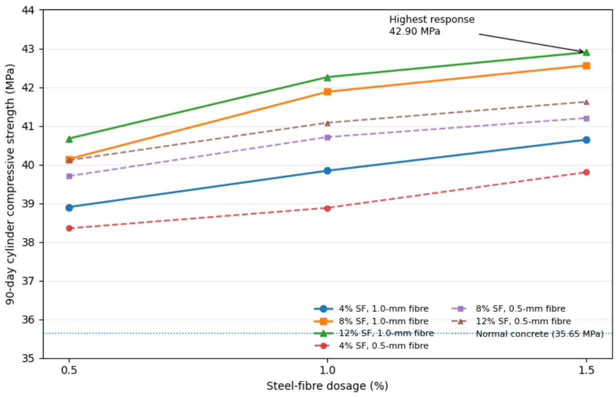

Figure 3 Combined influence of silica-fume replacement, steel-fibre dosage and fibre diameter on 90-day cylinder compressive strength.

As shown in Fig. 3, 90-day cylinder compressive strength increased consistently with fibre dosage across all silica-fume levels, while the 1.0-mm fibre series generally maintained higher strengths than the corresponding 0.5-mm series. The greatest response was obtained at 12% silica fume and 1.5% of the 1.0-mm fibre, confirming the combined contribution of matrix modification, fibre dosage and fibre geometry to compressive performance.

The results indicate that the effects of silica fume and steel fibres were complementary. Silica fume primarily strengthened and densified the matrix, whereas the fibres provided crack-bridging resistance. A denser matrix can also provide stronger fibre-matrix interaction, allowing stress to be transferred more effectively to the fibres. Similar combined effects have been reported in silica-fume/steel-fibre concretes, although the magnitude of compressive-strength improvement varies considerably with fibre geometry, fibre volume, matrix strength and workability.

The fact that compressive strength continued to rise up to 1.5% fibre in the present dataset should therefore be interpreted specifically within the tested mixture system. Other studies have found that excessive steel-fibre contents can reduce compressive strength when fibre clustering or poor compaction becomes dominant. Here, the use of progressively higher superplasticizer dosages appears to have prevented the workability reduction from becoming sufficiently severe to reverse the mechanical benefit.

4.4 Flexural behaviour and fibre efficiency

The influence of steel fibres was considerably more pronounced in flexure than would be expected from the compressive response alone. This difference is consistent with the fundamental reinforcing mechanism of discontinuous steel fibres. Under bending, fibres intersect developing cracks and transfer tensile stress across the crack plane. Their contribution therefore becomes increasingly important after matrix cracking begins.

For the 12% silica-fume mixtures containing 1.0-mm fibres, 28-day flexural strength increased from 5.88 MPa at 0.5% fibre to 6.16 MPa at 1.0% and 6.32 MPa at 1.5%. At 90 days, the corresponding values were 6.40, 6.67 and 6.85 MPa.

Table 4. Flexural strength of 12% silica-fume concrete reinforced with 1.0-mm steel fibres

Fibre dosage (%)	28 days (MPa)	90 days (MPa)	28-to-90-day gain (%)
0.5	5.88	6.40	8.84
1.0	6.16	6.67	8.28
1.5	**6.32**	**6.85**	8.39

Note: Percentage gains from 28 to 90 days are calculated from the experimental mean values.

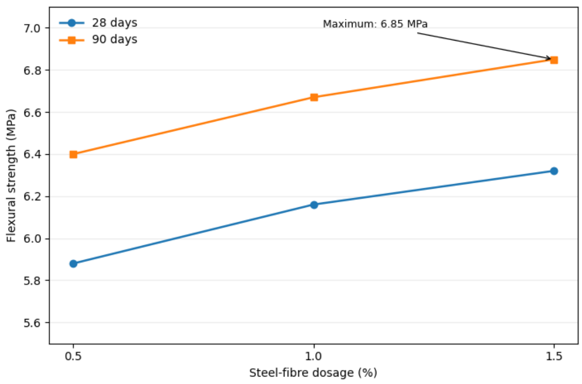

Figure 4 Effect of steel-fibre dosage on the flexural strength of concrete containing 12% silica fume and 1.0-mm-diameter steel fibres at 28 and 90 days.

As shown in Fig. 4, flexural strength increased consistently with steel-fibre dosage at both curing ages, with no indication of a reduction in performance up to the maximum investigated fibre content of 1.5%. The similar upward trends at 28 and 90 days indicate that the fibre-induced improvement was retained with continued curing, while the higher 90-day values reflect the additional contribution of matrix development.

The monotonic increase from 0.5 to 1.5% fibre indicates that the investigated range did not exceed the effective fibre content for flexural performance. Increasing the number of fibres increased the probability that a propagating crack would encounter one or more fibres capable of transferring stress across the crack. The original experimental observations also reported visibly different failure behaviour: fibre-reinforced beams remained more effectively connected after cracking, whereas normal concrete specimens separated much more readily following flexural failure.

This distinction between compressive and flexural behaviour is important. Steel fibres may produce only moderate gains in compressive strength while providing much larger improvements in tensile-controlled behaviour, toughness and crack resistance. Reviews of steel-fibre-reinforced concrete similarly identify crack bridging and post-cracking load transfer as the principal reasons for improved flexural behaviour.

The 90-day improvement relative to 28 days remained approximately 8–9% for all three fibre dosages. This indicates that later-age matrix development continued to contribute even after the fibres had been incorporated. The silica-fume-modified matrix therefore did not merely provide a higher initial flexural capacity; it continued to develop around the fibres with curing age.

The highest measured flexural strength within this series, **6.85 MPa**, occurred at 12% silica fume and 1.5% of the 1.0-mm steel fibre. This combination therefore coincides with the high-performance region identified from compressive strength, strengthening the case for a genuine interaction between silica-fume matrix enhancement and fibre reinforcement rather than an isolated improvement in one mechanical property.

4.5 Dynamic modulus of elasticity and ultrasonic pulse velocity

Dynamic modulus and ultrasonic pulse velocity provided complementary information on the internal quality and stiffness of the concrete. Both parameters increased with silica-fume replacement and further increased after steel-fibre incorporation, although the magnitude of the changes differed substantially.

For silica-fume concrete without fibres, the 28-day cylinder strength at 12% replacement was 36.78 MPa, accompanied by a dynamic modulus of 44.45 GPa and an average UPV of 4565 m/s. At 90 days, these values increased to 38.73 MPa, 45.86 GPa and 4603 m/s, respectively. The parallel increase in these responses indicates continued densification and stiffness development with curing.

The addition of fibres increased dynamic modulus further. For the 1.0-mm fibre series at 90 days, dynamic modulus rose from 43.06 GPa for normal concrete to 47.05 GPa with 4% silica fume and 1.5% fibre, 48.20 GPa with 8% silica fume and 1.5% fibre, and a maximum of **48.30 GPa** with 12% silica fume and 1.5% fibre.

A particularly useful observation emerges when the percentage improvements are compared. The optimum 12% SF–1.5% fibre mixture increased cylinder strength by **20.34%** and dynamic modulus by **12.16%**, but UPV increased by only **6.35%**. Thus, the relative improvement followed approximately:

compressive strength > dynamic modulus > UPV.

This difference is physically reasonable. UPV is strongly influenced by continuity, density, void structure and elastic wave transmission through the concrete, whereas strength is also affected by crack resistance and local stress redistribution. Steel fibres can substantially improve crack resistance without producing an equally large change in the bulk density or acoustic continuity of the material. Consequently, UPV should not be expected to increase in direct proportion to compressive strength.

Anusandhanvallari
Vol 2023, No.1
December 2023
ISSN 2229-3388

The experimental data nevertheless demonstrate a clear positive relationship between cylinder compressive strength and dynamic modulus. Depending on silica-fume content, fibre diameter and curing age, the reported regression coefficients for this relationship generally produced values between approximately **0.82 and 0.97**. For the 1.0-mm fibre series at 90 days, values of 0.952, 0.968 and 0.962 were obtained for 4, 8 and 12% silica fume, respectively. These high coefficients indicate that stiffness development tracked compressive-strength development closely within each mixture family.

4.6 Stress–strain response and static modulus of elasticity

The stress–strain response provides a more complete description of the effect of steel fibres than ultimate strength alone. Cylindrical specimens were tested at 28 and 90 days, and deformation was recorded using a compressometer. Stress–strain curves were obtained for normal concrete, silica-fume concrete and fibre-reinforced silica-fume concrete across the investigated fibre contents and diameters.

The experimental curves show that silica-fume incorporation shifted the response toward higher stress levels relative to normal concrete, reflecting the stronger cementitious matrix. Subsequent fibre addition increased the load-carrying capacity further and altered the cracking response. The fibre-reinforced specimens exhibited more distributed cracking than the normal concrete specimens. The original observations specifically note that cracking became more uniformly distributed with fibre addition at all investigated fibre percentages.

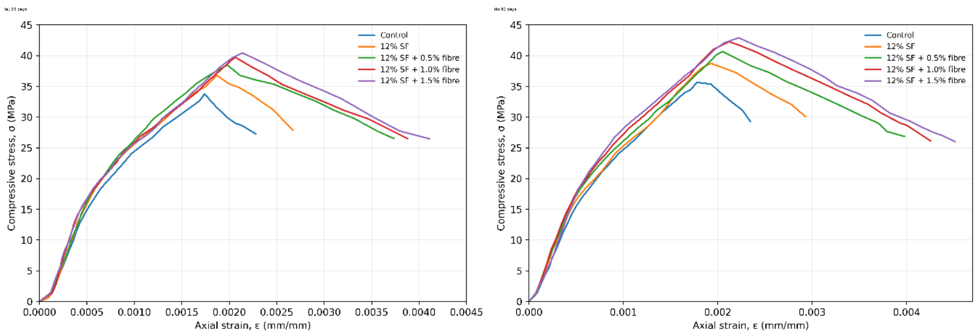

Figure 5 Representative compressive stress–strain response of normal concrete and concrete containing 12% silica fume with 0.5, 1.0 and 1.5% of 1.0-mm-diameter steel fibres at (a) 28 days and (b) 90 days

As shown in Fig. 5, the incorporation of silica fume shifted the stress–strain response above that of the control concrete, while subsequent steel-fibre addition progressively increased both the peak stress and the corresponding strain capacity. The fibre-reinforced mixtures also exhibited a more extended post-peak response, particularly at higher fibre dosages, indicating improved deformation capacity and crack-bridging action after attainment of the peak stress.

This behaviour is central to the mechanical role of the steel fibres. Once microcracks begin to develop, randomly distributed fibres crossing the cracks provide bridging resistance and restrict rapid crack opening. Instead of deformation becoming concentrated immediately within one dominant crack, damage can be distributed over a larger region of the specimen. This mechanism explains why the contribution of fibres becomes more evident in flexural and post-cracking behaviour than in the initial compressive response.

The static modulus followed the same broad trend as the dynamic modulus: silica-fume incorporation increased matrix stiffness, while fibre reinforcement produced additional improvement. However, static and dynamic moduli should not be regarded as interchangeable. The dynamic modulus is obtained from very small elastic disturbances and therefore does not involve significant crack development, whereas the static modulus reflects the actual deformation of the concrete under progressively applied mechanical loading. The latter is consequently more sensitive to microcracking and fibre-mediated crack restraint.

The combined results therefore show that the silica fume and fibres perform different but complementary functions. Silica fume improves the quality and strength of the cementitious matrix, while steel fibres modify the manner in which that matrix responds once cracking develops. The experimentally observed improvement in cracking characteristics, together with the increase in flexural strength and elastic properties, supports this interpretation.

More broadly, the mechanical response cannot be reduced to the statement that "more fibre produces stronger concrete." Fibre dosage, fibre geometry and matrix quality act together. Research on steel-fibre-reinforced concrete has similarly shown that fibre geometry and volume fraction can materially alter mechanical efficiency, while the effectiveness of the fibres depends on their interaction with the surrounding cementitious matrix. In the present study, the strongest overall behaviour within the investigated domain consistently shifted toward the combination of **12% silica fume, 1.5% steel fibre and 1.0-mm fibre diameter**.

At the same time, this combination should not yet be declared the final statistically validated optimum. It is the **experimental maximum within the tested domain**. Confirmation of whether silica-fume level, fibre dosage, fibre diameter and their interactions exert statistically significant effects requires the factorial and regression analysis presented in the following sections. That distinction is important: the largest observed mean is not automatically a statistically defensible optimum.

4.7 Statistical significance and interaction effects

The experimental trends discussed in the preceding sections indicate that silica-fume content, fibre dosage and fibre diameter all affected the mechanical response of the concrete. However, comparison of mean values alone cannot determine whether these differences exceed the variability associated with replicate testing. A factorial analysis of variance was therefore performed using the individual experimental observations for the fibre-reinforced mixtures. Silica-fume content (SF), fibre volume fraction (Vf) and fibre diameter (df) were treated as fixed factors. Separate analyses were conducted at 28 and 90 days to avoid confounding mixture effects with the systematic development of the cementitious matrix with curing age.

The analysis of cube compressive strength showed a particularly strong influence of silica-fume content. At 28 days, the main effect of silica fume was highly significant ($F = 86.52$, $p < 0.001$), with a partial η^2 of 0.828. Fibre dosage was also significant ($F = 27.30$, $p < 0.001$), as was fibre diameter ($F = 30.76$, $p < 0.001$). The same hierarchy remained evident at 90 days, when silica fume produced $F = 88.07$ and partial $\eta^2 = 0.830$, compared with $F = 24.93$ for fibre dosage and $F = 28.22$ for fibre diameter.

Table 5. Factorial ANOVA for cube compressive strength

Source	28 days: F	28 days: p	Partial η^2	90 days: F	90 days: p	Partial η^2
Silica fume (SF)	86.52	<0.001	0.828	88.07	<0.001	0.830
Fibre dosage (Vf)	27.30	<0.001	0.603	24.93	<0.001	0.581
Fibre diameter (df)	30.76	<0.001	0.461	28.22	<0.001	0.439
SF × Vf	0.03	0.998	0.003	0.01	>0.999	0.001
SF × df	0.02	0.985	<0.001	<0.01	>0.999	<0.001
Vf × df	3.36	0.046	0.157	3.20	0.053	0.151
SF × Vf × df	0.01	>0.999	0.001	0.01	>0.999	0.001

Note: ANOVA was calculated from the individual replicate measurements contained in the experimental dataset. Statistical significance was evaluated at $p < 0.05$.

These results provide an important qualification to the experimental discussion. Although the highest compressive strengths occurred when high silica-fume and fibre contents were combined, the statistical evidence does not indicate a strong silica-fume × fibre-dosage interaction. Instead, the effects of silica fume and fibre dosage within the investigated domain were predominantly additive. This distinction is important because an experimental maximum produced by two constituents does not necessarily demonstrate statistical synergy.

A modest interaction between fibre dosage and fibre diameter was detected at 28 days ($p = 0.046$), with a partial η^2 of 0.157. At 90 days, the same interaction approached but did not reach the conventional 5% significance threshold ($p = 0.053$). This suggests that the benefit obtained by increasing fibre dosage depended to some extent on fibre geometry, particularly at the earlier age. The observation is consistent with the experimentally higher strengths obtained from the 1.0-mm fibre series at increasing fibre contents.

The statistical response was different for flexural strength. Here, fibre dosage rather than silica-fume content emerged as the dominant factor. At 28 days, fibre dosage produced $F = 20.76$ ($p < 0.001$, partial $\eta^2 = 0.536$), while fibre diameter produced $F = 28.25$ ($p < 0.001$, partial $\eta^2 = 0.440$). Silica-fume content remained statistically significant but produced a smaller effect ($F = 6.04$, $p = 0.005$, partial $\eta^2 = 0.251$). The same pattern persisted at 90 days.

Table 6. Factorial ANOVA for flexural strength

Source	28 days: F	28 days: p	Partial η²	90 days: F	90 days: p	Partial η²
Silica fume (SF)	6.04	0.005	0.251	5.90	0.006	0.247
Fibre dosage (Vf)	20.76	<0.001	0.536	17.73	<0.001	0.496
Fibre diameter (df)	28.25	<0.001	0.440	25.21	<0.001	0.412
SF × Vf	0.06	0.993	0.007	<0.01	>0.999	<0.001
SF × df	0.02	0.975	0.001	<0.01	>0.999	<0.001
Vf × df	0.89	0.421	0.047	0.33	0.722	0.018
SF × Vf × df	0.04	0.996	0.005	0.01	>0.999	0.001

Anusandhanvallari
Vol 2023, No.1
December 2023
ISSN 2229-3388

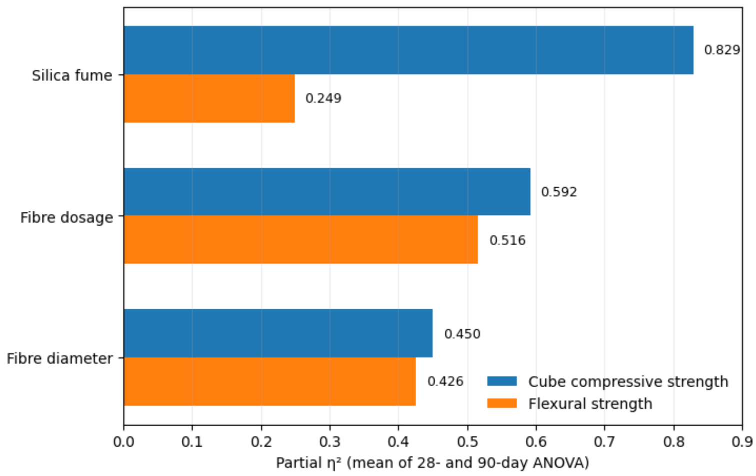

Figure 6 Comparison of the main-factor effect sizes on cube compressive and flexural strength based on mean partial η^2 values from the 28- and 90-day factorial ANOVA.

The difference between Tables 5 and 6 is mechanically meaningful. Silica fume was the dominant variable for compressive strength, whereas steel-fibre characteristics became considerably more influential in flexure. This supports the mechanisms discussed previously: silica fume primarily modifies the matrix, while fibres become increasingly important once tensile cracking and crack bridging control the response. Similar distinctions between compressive and flexural sensitivity to fibre reinforcement have been reported by Yazıcı, İnan, and Tabak (2007), Köksal et al. (2008), and Nili and Afroughsabet (2012).

The relative magnitudes of the main effects are illustrated in Fig. 6. Silica-fume content exerted the dominant influence on compressive strength, whereas its contribution to flexural strength was substantially smaller; in contrast, fibre dosage and fibre diameter showed comparatively stronger effects on the flexural response.

This distinction supports the proposed mechanical interpretation that silica fume primarily governs matrix-strength development, while steel-fibre characteristics become increasingly important when the response is controlled by tensile cracking and crack bridging.

The lack of significant higher-order interactions should not be hidden. On the contrary, it improves the interpretation of the experiment. Within the investigated range, the principal performance gains were governed mainly by strong main effects rather than complex three-factor interactions. Accordingly, the term synergistic in describing the combined system should refer to the complementary physical roles of matrix densification and crack bridging, rather than implying that all factors exhibited statistically significant synergistic interactions.

4.8 Predictive relationships and model performance

The experimental dataset was further examined to determine whether the measured properties could be related through empirical predictive relationships. Such relationships are useful because several properties of fibre-reinforced concrete are experimentally demanding to determine, whereas compressive strength is routinely available. A reliable correlation between compressive strength and flexural strength, elastic modulus or UPV can therefore provide useful preliminary estimates within the experimental domain.

The original experimental analysis developed separate linear relationships according to curing age, silica-fume level and fibre diameter. The relationship between cube compressive strength (fcf) and flexural strength (frf) was generally strong. For the 0.5-mm fibre series, R^2 values ranged from 0.897 to 0.963, while the 1.0-mm series produced values between 0.928 and 0.973 for most investigated combinations. The complete source data report, for example, an R^2 of 0.973 for the 28-day, 8% silica-fume, 1.0-mm fibre series.

Table 7. Representative predictive relationships from the experimental dataset

Predicted response	Age (days)	SF (%)	Fibre diameter (mm)	Representative equation	R^2
Flexural strength	28	8	1.0	$f_{rf} = 0.336 f_{cf} - 9.706$	0.973
Flexural strength	90	4	1.0	$f_{rf} = 0.359 f_{cf} - 10.71$	0.964
Cylinder compressive strength	90	12	0.5	$f_{fc} = 1.608 f_{cf} - 37.67$	0.977
Cylinder compressive strength	90	12	1.0	$f_{fc} = 1.478 f_{cf} - 31.44$	0.973
Dynamic modulus	90	8	1.0	$E_{df} = 0.628 f_{fc} + 21.52$	0.968
Dynamic modulus	90	12	1.0	$E_{df} = 0.562 f_{fc} + 24.18$	0.962
UPV	28	12	0.5	$UPV_f = 50.63 f_{fc} + 2691$	0.930
Static modulus	90	12	0.5	$E_{cf} = 0.501 f_{fc} + 12.71$	0.952

Note: Equations and R^2 values are reproduced from the mathematical relationships developed from the experimental dataset. The notation follows the original experimental model.

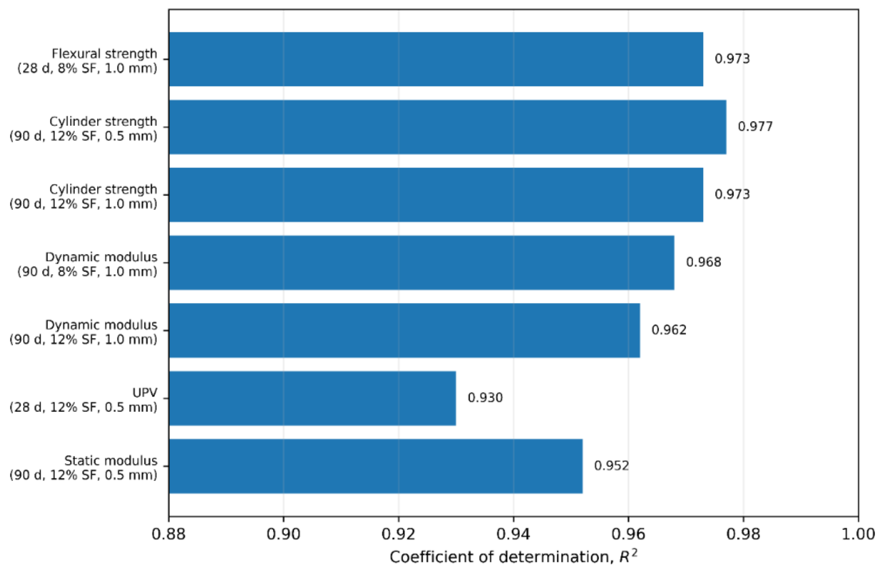

Figure 7 Comparison of the coefficient of determination (R^2) for representative predictive relationships developed from the experimental dataset.

As illustrated in Fig. 7, the developed relationships generally exhibited strong predictive agreement, with values ranging from 0.930 to 0.977 for the representative models. The strongest relationship was obtained for the prediction of 90-day cylinder compressive strength at 12% silica fume and 0.5-mm fibre diameter (), while the comparatively lower for UPV indicates greater variability in relating acoustic response to mechanical strength.

The relationship between cube and cylinder compressive strength was particularly strong. Depending on mixture condition, the cylinder-strength models yielded R^2 values approaching 0.98. This indicates that the two compressive-strength measurements responded similarly to silica-fume and fibre modification, despite differences in specimen geometry and stress distribution.

Dynamic modulus also showed a strong relationship with cylinder compressive strength. For the 1.0-mm fibre mixtures at 90 days, R^2 values of 0.952, 0.968 and 0.962 were obtained at silica-fume contents of 4, 8 and 12%, respectively. These values are consistent with the earlier experimental observation that compressive strength and dynamic modulus increased in parallel as the matrix became denser and the fibre content increased.

The UPV relationships produced R^2 values of approximately 0.89–0.93 across the investigated combinations. Although these correlations are reasonably strong, they should not be interpreted as evidence that UPV is a direct substitute for compressive-strength testing. The magnitude of the UPV increase was substantially smaller than the strength increase. At 12% silica fume and 1.5% of the 1.0-mm fibre, for example, the 90-day compressive strength increased by 20.34% relative to normal concrete, whereas UPV increased by only 6.35%. Thus, the relationship is useful for comparative prediction within the investigated system but does not imply identical sensitivity to mixture modification.

Static modulus was less consistently predicted from compressive strength, particularly at 28 days. The original models produced R^2 values as low as approximately 0.71 for some combinations but considerably higher values at 90 days. This weaker early-age relationship probably reflects the greater sensitivity of static deformation to microcracking and local heterogeneity. Dynamic measurements involve very small strains, whereas static modulus is determined during mechanical loading and is therefore more sensitive to the onset and development of microcracking.

This variation in predictive accuracy reinforces the need for property-specific models. A single compressive-strength equation cannot be assumed to predict flexural strength, static stiffness, dynamic stiffness and acoustic response with equal reliability. Recent research has increasingly adopted response-surface and machine-learning approaches for precisely this reason, particularly when fibre geometry and supplementary cementitious materials are considered simultaneously. However, complex modelling is only useful when supported by sufficiently large and independent datasets. With the present experimental dataset, transparent regression relationships remain more defensible than introducing an unnecessarily complex machine-learning model.

The original study also compared its predictive models with experimental observations from external studies. Its validation dataset reported that most observations remained within the adopted prediction limits, although deviations occurred for some external combinations. This provides useful evidence that the relationships capture broad mechanical trends, but it should not be interpreted as universal validation because concrete constituent properties and fibre characteristics vary substantially among independent experimental programmes.

Accordingly, the equations developed here should be treated as empirical models valid primarily within the investigated range of silica-fume replacement, fibre dosage, fibre geometry and concrete strength. Extrapolation beyond those limits would require independent experimental validation.

Anusandhanvallari
Vol 2023, No.1
December 2023
ISSN 2229-3388

4.9 Integrated performance assessment and optimum mixture

Determining an optimum mixture solely from compressive strength would ignore the principal reason for introducing steel fibres. The experimental programme therefore requires an integrated assessment that considers fresh-state behaviour, compressive and flexural strength, elastic properties, UPV and cracking behaviour together.

The results reveal a consistent progression toward higher mechanical performance as silica-fume replacement increased from 4 to 12%, fibre dosage increased from 0.5 to 1.5%, and the fibre diameter changed from 0.5 to 1.0 mm. Importantly, silica-fume-only testing showed that this progression could not be extended indefinitely: increasing silica fume beyond 12% to 16% caused cube compressive strength to decline. Thus, the upper silica-fume level used in the fibre-reinforced factorial programme corresponds closely to the experimentally identified optimum matrix composition.

Among the fibre-reinforced mixtures, 12% silica fume + 1.5% steel fibre + 1.0-mm fibre diameter produced the strongest overall performance within the tested experimental domain.

Table 8. Integrated assessment of the experimentally best-performing mixture

Performance indicator	Reference / lower condition	12% SF + 1.5% fibre + 1.0-mm fibre	Interpretation
90-day cylinder compressive strength	35.65 MPa	42.90 MPa	+20.34%
90-day dynamic modulus	43.06 GPa	48.30 GPa	+12.16%
90-day UPV	4468 m/s	4752 m/s	+6.35%
28-day flexural strength*	5.08 MPa	6.32 MPa	+24.4%
90-day flexural strength*	5.41 MPa	6.85 MPa	+26.6%
Fresh-state demand	Lower SP demand	Highest SP region	Workability penalty
Cracking behaviour	More localised cracking	More distributed cracking	Improved crack control

**Flexural percentage improvements calculated relative to the corresponding normal-concrete mean.*

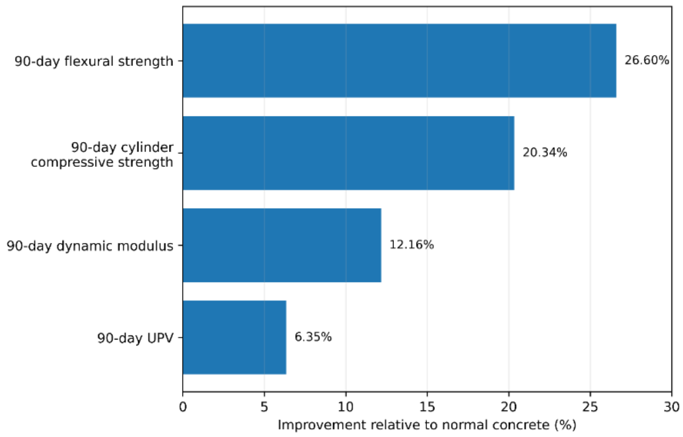

Figure 8 Relative improvement in the principal hardened-concrete properties of the best-performing mixture (12% silica fume + 1.5% steel fibre + 1.0-mm fibre diameter) compared with normal concrete.

The improvement in flexural strength is particularly noteworthy. Relative to normal concrete, the selected mixture increased flexural strength by approximately 24.4% at 28 days and 26.6% at 90 days. This increase exceeded the relative improvement observed in compressive strength, confirming that the principal mechanical benefit of fibre incorporation lies in tensile-controlled and cracking-sensitive behavior rather than simple enhancement of matrix compressive capacity.

The same mixture also produced the highest dynamic modulus and UPV within the reported 1.0-mm fiber series. However, the magnitude of these improvements differed markedly. The 20.34% increase in cylinder compressive strength was accompanied by a 12.16% increase in dynamic modulus and only a 6.35% increase in UPV. This hierarchy demonstrates that different response variables capture different aspects of composite behaviour and supports the use of a multi-response assessment rather than a single-property optimisation criterion.

Statistical results strengthen this interpretation but also impose an important qualification. The experimental maximum occurred at the upper levels of all three investigated factors, yet factorial ANOVA showed that silica-fume content, fibre dosage and fibre diameter were predominantly significant main effects. Most interaction terms were not statistically significant. Consequently, the optimum should be described as the best-performing combination within the experimentally investigated domain, rather than as proof of a strong three-factor statistical synergy.

There is also a practical cost to this mechanical improvement. The high-performance mixtures required progressively greater superplasticizer dosage to compensate for reduced workability. The 1.0-mm fibre series containing 12% silica fume and 1.5% fibre required approximately 1.8% superplasticizer, while slump remained only about 22 mm. Increasing fibre or silica-fume content beyond the investigated range could therefore produce diminishing mechanical returns while creating increasingly difficult mixing, dispersion and placement conditions.

From an engineering perspective, this means that the optimum depends on the intended application. If maximum mechanical and crack-control performance is the principal objective, the 12% SF–1.5% fibre–1.0-mm combination is the preferred mixture within the present experimental space. If workability, fibre consumption and admixture demand are given greater weight, a lower fibre dosage may provide a more economical compromise. For example, at 12% silica fume and 1.0% of the 1.0-mm fibre, 90-day cylinder strength had already reached 42.26 MPa, only 1.5% below the 42.90 MPa obtained at 1.5% fibre. This indicates diminishing marginal gains in compressive strength between 1.0 and 1.5% fibre, even though flexural and cracking performance continued to benefit from the higher fibre dosage.

This distinction is valuable for practical mixture design. The composition that maximises every measured mechanical response is not necessarily the composition that provides the greatest performance gain per unit of fibre or chemical admixture. Future optimisation should therefore incorporate material cost, embodied environmental impact and workability alongside mechanical performance.

Overall, the experimental and statistical evidence demonstrates that the three design variables do not contribute equally to all properties. Silica-fume content dominates the compressive-strength response; fibre dosage and fibre geometry exert proportionally greater influence on flexural performance; and stiffness and UPV occupy an intermediate response regime. The combination of 12% silica fume and 1.5% steel fibre with the 1.0-mm fibre produced the highest overall measured performance, while the statistical analysis shows that this outcome results mainly from the cumulative effects of matrix enhancement and fibre reinforcement rather than a universally significant higher-order interaction.

This distinction provides a more defensible interpretation of silica-fume steel-fibre concrete than selecting an optimum from compressive strength alone and is consistent with the broader understanding that fibre-reinforced cementitious composites must be evaluated through multiple mechanical responses (Köksal et al. 2008; Nili and Afroughsabet 2012; Ramadoss et al. 2022).

5. Conclusions

This study examined the combined influence of silica-fume replacement, steel-fibre dosage and fibre diameter on the fresh, mechanical, elastic and nondestructive response of concrete. The experimental programme considered silica-fume replacement levels of 4, 8 and 12%, steel-fibre dosages of 0.5, 1.0 and 1.5%, and fibre diameters of 0.5 and 1.0 mm, with performance evaluated primarily at 28 and 90 days.

The results showed that silica fume produced a clear improvement in compressive strength up to a replacement level of approximately 12%. At 28 days, cube compressive strength increased from 40.37 MPa for the reference concrete to 45.18 MPa at 12% silica fume, while the corresponding 90-day strength increased from 42.16 to 47.48 MPa. Increasing silica-fume replacement further to 16% reduced strength, confirming that the beneficial effect was not proportional to dosage and that the optimum matrix region occurred near 12% replacement.

Steel-fibre addition provided further improvements, particularly at higher fibre contents. For the 1.0-mm fibre series, the combination of 12% silica fume and 1.5% steel fibre produced a 90-day cylinder compressive strength of 42.90 MPa, compared with 35.65 MPa for normal concrete, corresponding to an increase of 20.34%. The same mixture reached a dynamic modulus of 48.30 GPa and an UPV of 4752 m/s, representing improvements of 12.16 and 6.35%, respectively.

The fibre contribution was even more pronounced in flexure. At 12% silica fume with 1.0-mm-diameter fibres, 90-day flexural strength increased from 6.40 MPa at 0.5% fibre to 6.85 MPa at 1.5% fibre. The stress–strain response also showed higher peak stress, increased strain capacity and a more extended post-peak response with fibre incorporation, consistent with improved crack bridging and more distributed cracking.

Factorial ANOVA confirmed that the experimental variables did not influence all responses equally. Silica-fume content was the dominant factor governing cube compressive strength, whereas fibre dosage and fibre diameter exerted comparatively stronger effects on flexural performance. Most higher-order interaction terms were not statistically significant, indicating that the observed gains were governed mainly by strong main effects rather than a universal three-factor synergy.

Within the investigated experimental domain, **12% silica fume + 1.5% steel fibre + 1.0-mm fibre diameter** produced the highest overall measured performance. However, the gain in compressive strength from increasing fibre dosage from 1.0 to 1.5% was relatively small compared with the additional fibre and superplasticizer demand, indicating diminishing marginal benefit at the upper dosage level. The selected combination should therefore be regarded as the **best-performing mixture within the tested range**, rather than a universally optimal composition.

Overall, the study demonstrates that silica fume primarily enhances matrix strength and stiffness, while steel fibres exert a stronger influence on flexural response, deformation capacity and crack control. A multi-response assessment is therefore more appropriate than optimisation based on compressive strength alone. Future work should incorporate complete material-characterisation data, cost and environmental indicators, and independent validation of the predictive relationships to improve the practical applicability of the proposed framework.

References:

[1] **Köksal, F., Altun, F., Yiğit, İ., & Şahin, Y. (2008).** *Combined effect of silica fume and steel fiber on the mechanical properties of high strength concretes.* **Construction and Building Materials, 22(8), 1874–1880.** DOI: 10.1016/j.conbuildmat.2007.04.017. **Critical paper for us.** It considers silica fume, fibre volume and two fibre aspect ratios.

[2] **Bayasi, Z., & Soroushian, P. (1997).** *Effect of silica fume and steel fibers on some properties of high-strength concrete.* **Construction and Building Materials, 11(7–8), 373–382.** DOI: 10.1016/S0950-0618(97)00058-5.

[3] **Nili, M., & Afroughsabet, V. (2012).** *Property assessment of steel-fibre reinforced concrete made with silica fume.* **Construction and Building Materials, 28(1), 664–669.** DOI: 10.1016/j.conbuildmat.2011.10.027.

[4] **Nili, M., & Afroughsabet, V. (2010).** *Combined effect of silica fume and steel fibers on the impact resistance and mechanical properties of concrete.* **International Journal of Impact Engineering, 37(8), 879–886.** DOI: 10.1016/j.ijimpeng.2010.03.004.

[5] **Yan, H., Sun, W., & Chen, H. (1999).** *The effect of silica fume and steel fiber on the dynamic mechanical performance of high-strength concrete.* **Cement and Concrete Research, 29(3), 423–426.** DOI: 10.1016/S0008-8846(98)00235-X.

[6] **Behnood, A., & Ghandehari, M. (2009).** *Comparison of compressive and splitting tensile strength of high-strength concrete with and without polypropylene fibers heated to high temperatures.* **Fire Safety Journal.**
Useful background for fibre-modified HSC behaviour.

[7] **Afroughsabet, V., & Ozbakkaloglu, T. (2015).** *Mechanical and durability properties of high-strength concrete containing steel and polypropylene fibers.* **Construction and Building Materials, 94, 73–82.** DOI: 10.1016/j.conbuildmat.2015.06.051. Silica fume was incorporated in the mixes.

[8] **Ali, B., Raza, S. S., Hussain, I., & Iqbal, M. (2021).** *Influence of different fibers on mechanical and durability performance of concrete with silica fume.* **Structural Concrete, 22(1), 318–333.** DOI: 10.1002/suco.201900422.

[9] **Zhang, H., Cao, L., Duan, Y., Tang, Z., & Hu, F. (2022).** *High-flowable and high-performance steel fiber reinforced concrete adapted by fly ash and silica fume.* **Case Studies in Construction Materials.** Particularly useful for explaining fibre–matrix interaction and flowability.

[10] **Ramadoss, P., Li, L., Fatima, S., & Sofi, M. (2022).** *Mechanical performance and numerical simulation of high-performance steel fiber reinforced concrete.* **Journal of Building Engineering.** DOI: 10.1016/j.jobe.2022.105424. Uses 10–15% silica fume, two fibre aspect ratios and 0–1.5% fibre volume, making it **extremely relevant** to our work.

[11] **Singh, G. (2021).** *Study on collective effect of silica fume and steel fiber on strength and durability properties of concrete.* **Materials Today: Proceedings, 37, 2256–2265.** DOI: 10.1016/j.matpr.2020.07.701.

[12] **Wu, Z., Shi, C., & Khayat, K. H. (2016).** *Influence of silica fume content on microstructure development and bond to steel fiber in ultra-high strength cement-based materials.* **Cement and Concrete Composites, 71, 97–109.** DOI: 10.1016/j.cemconcomp.2016.05.005.

[13] **Chan, Y. W., & Chu, S. H. (2004).** *Effect of silica fume on steel fiber bond characteristics in reactive powder concrete.* **Cement and Concrete Research, 34(7), 1167–1172.** DOI: 10.1016/j.cemconres.2003.12.023. Excellent mechanistic citation for fibre–matrix bonding.

[14] **Özalp, F., Yılmaz, H. D., & Akçay, B. (2022).** *Mechanical properties and impact resistance of concrete composites with hybrid steel fibers.* **Frontiers of Structural and Civil Engineering, 16, 615–623.** DOI: 10.1007/s11709-022-0828-y.

[15] **Use of silica fume and recycled steel fibers in self-compacting concrete (SCC) (2016). Construction and Building Materials, 125, 196–209.** DOI: 10.1016/j.conbuildmat.2016.08.046.

[16] **Yazıcı, Ş., İnan, G., & Tabak, V. (2007).** *Effect of aspect ratio and volume fraction of steel fiber on the mechanical properties of SFRC.* **Construction and Building Materials, 21(6), 1250–1253.** DOI: 10.1016/j.conbuildmat.2006.05.025.
Essential reference. It considers , , strength and UPV—the comparison with our dataset is obvious.

[17] **Song, P. S., & Hwang, S. (2004).** *Mechanical properties of high-strength steel fiber-reinforced concrete.* **Construction and Building Materials, 18(9), 669–673.** DOI: 10.1016/j.conbuildmat.2004.04.027.

[18] **Gao, J., Sun, W., & Morino, K. (1997).** *Mechanical properties of steel fiber-reinforced, high-strength, lightweight concrete.* **Cement and Concrete Composites, 19(4), 307–313.** DOI: 10.1016/S0958-9465(97)00023-1.

[19] **Evaluation of mechanical properties of steel fiber reinforced concrete with different strengths of concrete (2018). Construction and Building Materials, 168, 556–569.** DOI: 10.1016/j.conbuildmat.2018.02.164.

[20] **Effects of steel fiber length and coarse aggregate maximum size on mechanical properties of steel fiber reinforced concrete (2019). Construction and Building Materials.** Useful for separating fibre length/geometry effects from dosage effects.

[21] **Tiberti, G., Germano, F., Mudadu, A., & Plizzari, G. A. (2018).** *An overview of the flexural post-cracking behavior of steel fiber reinforced concrete.* **Structural Concrete, 19, 695–718.** DOI: 10.1002/suco.201700068.

[22] **Gali, S., & Subramaniam, K. V. L. (2017).** *Evaluation of crack propagation and post-cracking hinge-type behavior in the flexural response of steel fiber reinforced concrete.* **International Journal of Concrete Structures and Materials, 11, 365–375.** DOI: 10.1007/s40069-017-0197-4.

[23] **Barros, J. A. O., Cunha, V. M. C. F., & Ribeiro, A. F. (2005).** *Post-cracking behaviour of steel fibre reinforced concrete.* **Materials and Structures, 38, 47–56.** DOI: 10.1007/BF02480574.

[24] **Predicting the post-cracking behavior of normal- and high-strength steel-fiber-reinforced concrete beams (2015). Construction and Building Materials, 93, 477–485.** DOI: 10.1016/j.conbuildmat.2015.06.006.

[25] **Post-cracking behaviour of steel and macro-synthetic fibre-reinforced concretes (2011). Construction and Building Materials, 25(5), 2713–2722.** DOI: 10.1016/j.conbuildmat.2010.12.022.

[26] **The influence of steel fiber tensile strengths and aspect ratios on the fracture properties of high-strength concrete (2019).** Relevant for fibre aspect ratio, fracture energy and toughness.

[27] **Mechanical and physical characterisation of steel fibre reinforced self-compacting concrete: Different aspect ratios and volume fractions of fibres (2022). Results in Engineering, 13, 100335.** DOI: 10.1016/j.rineng.2022.100335.

[28] **Effects of steel fiber percentage and aspect ratios on fresh and hardened properties of ultra-high performance fiber reinforced concrete (2021). Applied Mechanics, 2, 501–515.** DOI: 10.3390/applmech2030028.

[29] **Modelling and experimental validation of flexural tensile properties of steel fiber reinforced concrete (2021). Construction and Building Materials.** Particularly relevant to the predictive-model component.

[30] **Zheng, Y., Lv, X., Hu, S., Zhuo, J., Wan, C., & Liu, J. (2022).** *Mechanical properties and durability of steel fiber reinforced concrete: A review.* **Journal of Building Engineering.** DOI: 10.1016/j.jobe.2022.108025.

[31] **Siddique, R. (2011).** *Utilization of silica fume in concrete: Review of hardened properties.* **Resources, Conservation and Recycling, 55(11), 923–932.** DOI: 10.1016/j.resconrec.2011.06.012.

[32] **Siddique, R. (2011).** *Utilization of silica fume in concrete: Review of durability properties.* **Resources, Conservation and Recycling, 57, 30–35.** DOI: 10.1016/j.resconrec.2011.09.016.

[33] **An overview of mechanical, permeability, and thermal properties of silica fume concrete using bibliographic survey and building information modelling (2022). Construction and Building Materials, 385, 131489.** DOI: 10.1016/j.conbuildmat.2022.131489. Particularly valuable because its review places typical optimum silica-fume content around **7.5–12%**, which directly overlaps our 4–12% experimental range.

[34] **Singh, A., & Singh, N. (2022).** *Mechanical properties of silica fume based concrete: A review.* **Materials Today: Proceedings.** DOI: 10.1016/j.matpr.2022.05.037.

[35] **Performance characteristics of cementitious composites modified with silica fume: A systematic review (2022). Case Studies in Construction Materials, 18, e01753.** DOI: 10.1016/j.cscm.2022.e01753.

[36] **Effect of silica fume on the properties of sustainable cement concrete (2022). Journal of Materials Research and Technology, 24, 8887–8908.** DOI: 10.1016/j.jmrt.2022.05.147.

[37] **Mechanical properties of silica fume based concrete: A review (2022).** Use specifically for current consensus regarding optimum SF ranges and research gaps.

[38] **Wu, Z., Shi, C., & Khayat, K. H. (2016).** *Influence of silica fume content on microstructure development and bond to steel fiber in ultra-high strength cement-based materials.* **Cement and Concrete Composites, 71, 97–109.** This paper deserves citation in both the silica-fume mechanism and fibre-interface discussions.

[39] **Optimization based on toughness and splitting tensile strength of steel-fiber-reinforced concrete incorporating silica fume using response surface method (2022). Materials, 15, 6218.** This is probably our **single most important statistical comparison paper** because SF content, fibre volume and aspect ratio were all independent variables.

[40] **Machine learning-based prediction for compressive and flexural strengths of steel fiber-reinforced concrete (2021). Construction and Building Materials, 266, 121117.** DOI: 10.1016/j.conbuildmat.2020.121117. Particularly important because silica-fume content emerged as an influential predictor.

[41] **Statistical analysis and preliminary study on the mix proportion design of self-compacting steel fiber reinforced concrete (2019).** Statistical analysis based on **301 experimental datasets**, including fibre type, aspect ratio and volume fraction.

[42] **Modeling and optimization of the mechanical properties of fibre reinforced concrete containing silica fume using response surface methodology (2022). Case Studies in Construction Materials, 17, e01633.** Useful methodologically for RSM construction and validation.

[43] **Ramadoss et al. (2022).** *Mechanical performance and numerical simulation of high-performance steel fiber reinforced concrete.* **Journal of Building Engineering.** Uses empirical equations, ANFIS and multiple linear regression.

[44] **Yazıcı et al. (2007).** *Effect of aspect ratio and volume fraction of steel fiber on mechanical properties of SFRC.* Besides being experimentally relevant, this study used **multiple linear regression** to relate fibre parameters to strength.

[45] **Song & Hwang (2004).** *Mechanical properties of high-strength steel fiber-reinforced concrete.* Includes predictive strength relationships in addition to the experimental programme.

[46] **Mechanical and environmental performance evaluation of metakaolin and silica fume-modified steel fiber embedded concrete: A sustainable construction (2022).** Uses **RSM** and evaluates compressive, tensile, flexural, modulus and UPV responses. This is extremely important because reviewers may compare our analytical contribution directly against studies like this.

[47] **Guo, Y., Lu, Q., Du, G., & Zhang, J. (2022).** *Mechanical properties of concrete with low-content rubber particles co-reinforced by silica fume and steel fiber under freeze-thaw cycles.* **Construction and Building Materials, 490, 142515.** DOI: 10.1016/j.conbuildmat.2022.142515.

[48] **Influence of steel fiber type, content, and dimensions on compressive strength and ultrasonic pulse velocity of high-performance concrete (2022). Multiscale and Multidisciplinary Modeling, Experiments and Design, 9, 147.** Particularly relevant to our UPV/fibre-geometry analysis.

[49] **A study on the influencing factors of the mechanical properties of steel-fiber-reinforced cement concrete (2022). Materials, 19, 1493.** Examines fibre type, aspect ratios of 40–60 and contents of 0.5–1.5%.

[50] **Predictive modelling and comparative evaluation of residual flexural strengths of steel fibre-reinforced concrete (2022). Materials and Structures.** Uses a database of **1,645 flexural tests across 365 SFRC mixes** and identifies fibre volume, compressive strength and aspect ratio as dominant predictive variables. This is valuable for positioning our predictive modelling against current research.